JOURNAL OF MATERIALS SCIENCE **34** (1999) 4995–5004

Tribological behaviour and acoustic emissions of alumina, silicon nitride and SAE52100 under dry sliding

H. S. BENABDALLAH, R. J. BONESS
Department of Mechanical Engineering, Royal Military College of Canada, PO Box 17000 Stn Forces, Kingston, Ontario, Canada, K7K 7B4
E-mail: benabdallah-h@rmc.ca

The friction, wear and acoustic emission behaviour of various combinations of alumina, silicon nitride, and SAE52100 steel, operating under dry sliding conditions, was investigated. A designed ball-on-flat-disc type of tribometer was used to conduct these experiments. This apparatus, equipped with a force sensor, using silicon strain gauges, measured simultaneously the normal load and friction force. Both forces were used to determine the real-time value of the dynamic coefficient of friction. The AE signal arising from the interaction of the surfaces in dynamic contact was also detected and a data acquisition system was used to gather this signal as well as the outputs from the force sensor, at high frequency. The effects of test duration, sliding speed and normal load on the above mentioned tribological parameters were evaluated. The interest of this study further extended to assess the correlations that may exist between the integrated rms acoustic signal (AE) and the friction mechanisms, wear volume, friction work as well as the material removal power. Under the specific conditions of the present experiments, no consistent relation was found between the variations of AE and corresponding dynamic coefficient of friction (COF) as function of time. The variation of COF and wear rate, obtained considering a fixed total sliding distance of 500 m, as function of a range of sliding speed (0.05–2.5 m/s) and normal load (5–40 N) are presented. It was found that the test duration has an important impact on wear results of the experiments conducted at different sliding speeds and fixed travelling distance. More expected behaviour was observed when the relationships between the AE and wear volume, friction work, and material removal power were investigated considering the data obtained at different loadings and fixed sliding speed. Some models representing interesting relationships which could be used for predicting tribological properties in the case of practical applications, similar to the tribo-systems investigated in this study, are proposed.

1. Introduction

Many studies have so far been carried out to investigate the friction and wear behaviour of different ceramic materials when in dynamic contact with themselves or with metallic surfaces especially hard steel. Various tribological conditions have been considered with a focus on the effect of the testing environment (dry, humid, lubricated with water, alcohol or conventional lubricants also with additives). The majority of experimental set-ups used were in the from of pin-on-disc arrangements equipped in some cases with features that allow the removal from the contact zone of wear debris generated during sliding. Despite the considerable effort undertaken by the researchers some conflicting and sometimes unexpected results were found which did not contribute to finding useful correlations, between the friction and wear properties, and the operating conditions, that characterize these materials. Although, the literature does reveal a good understanding of the mechanisms of wear in sliding contacts and how these mechanisms are affected by the variation of the operating conditions. It is recognized that under moderate load and sliding speed conditions ceramics exhibit mild wear, characterized by essentially microcracking of the sub-surface. In some situations increasing the contact parameters can produce severe wear regimes with a drastic increase of the wear rate [1]. Alternatively, layers of low mechanical strength formed from compacted smaller fragments and particles [2] or more coherent thin layers of enhanced mechanical properties can protect the rubbing surfaces. In the case of silicon nitride, these layers are mainly composed of oxidation elements. This tribochemical reaction responsible for the oxidation occurs even at room temperature with an obvious effect of the humidity of the environment as reported among others by Lancaster

et al. [3]. Plastic flow phenomenon was also revealed by worn surfaces of silicon nitride, despite their known brittle behaviour, attributed to the decrease of the yield strength of the material due to high temperature generation at the contact during sliding. In a ceramic-steel sliding contact, hard debris of carbide so formed act as abrasive particles of the steel surface but at the same time any accumulation of these particles can be beneficial in separating the contacting surfaces [4]. In general it is well known that friction and wear depend on the properties and configuration of the entire tribosystem as well as measurement techniques of the different parameters, characteristics of the tribometer (vibrations, precision of its mechanical parts), materials in contact and the environment. The range of dynamic coefficient of friction reported so far for ceramics varies between as low as 0.1 and even slightly higher than 1.0, while the wear rate has a magnitude of about 10^{-5} $mm^3/N/m$ with a marked influence of the sliding speed. The literature reports that silicon nitride is a good candidate to be used in sliding applications in air.

The aim of the present study is the investigation of the influence of individual test parameters such as sliding speed, normal load, test duration on the friction, wear and acoustic emission properties in the case of continuous dry sliding for four materials combinations namely Si_3N_4/Si_3N_4, Al_2O_3/Si_3N_4, Si_3N_4/SAE52100 steel and Al_2O_3/SAE52100. Any tested combination will be referred to hereafter by the two considered materials the first being always the ball (sample) the second being the disc. It is believed that this work would contribute to understanding the tribological process that occurs under the selected conditions and the generation of some reproducible data. The interest in the acoustic emission (AE) generated from sliding contact processes involving ceramic materials is relatively new and most efforts in this field have so far been dedicated to studying metallic materials under dry or lubricated conditions [5, 6].

2. Experimental procedure, samples preparation and materials

The designed apparatus used in this study is shown in Fig. 1. Configured as ball-on-disc, it is powered by a 1 kW brushless motor equipped with a servo amplifier and controlled by a computer. This assembly provides the rotating movement and torque to the disc through a flexible coupling that prevents vibrations from being transmitted to the tribo-system. Sliding speeds corresponding to a range of rotating speeds varying between 1 and 1400 rpm can be obtained with an accuracy equivalent to ± 0.1 rpm. The sample (ball) holder is attached to a very rigid arm which is linked to the rig support by means of a horizontal pivot, mounted on precision bearings, whose axis lies in the interfacial plane of initial contact between the ball and the disc and thus eliminating any moment that would otherwise be created by the friction force in dynamic state. The arm is balanced by a counterweight. Care was taken in order to ensure that the arm was perfectly horizontal at the beginning of each test. A force sensor equipped with silicon strain gauges was used to measure simultaneously the normal load and friction force with a resolution of at least 0.05 N. It should be pointed out that although a dead weight was utilized to apply the normal load, due to inertia effects the instantaneous values of this force was not constant during testing. The corresponding friction force and normal force measured by the sensor, were adopted in the calculation of the realtime value of the dynamic coefficient of friction. The signals from the sensor were filtered and amplified by a controller whose

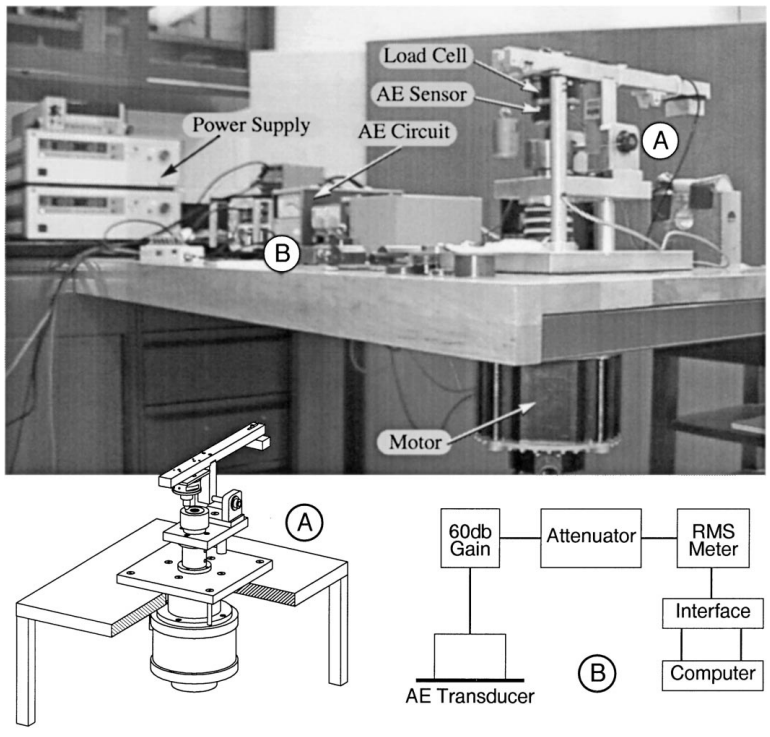

Figure 1 Tribometer in operation and diagram of acoustic emission circuit.

outputs were fed into a computer through a 12 bits data acquisition board that could sample simultaneously all channels at a frequency range of 1 to 1000 Hz. This controller contains also a biasing internal software that provides a way to offset the output signals at the beginning of the test.

Generally, AE signals fall into two categories: transient pulses (burst emissions) and pseudocontinuous emissions. The most common measurements used for burst emissions is what is known as ringdown counts which consists of counting the number of times the amplified AE signal crosses a preset trigger level voltage. The second category was selected for the present study without considering any threshold level for measurement of AE signals. Accordingly, the AE signal arising from the interaction of the surfaces in dynamic contact was detected by means of an acoustic emission transducer with a resonant frequency of 750 kHz acoustically coupled to the sample (ball) holder with silicon grease. The signal from the transducer was fed into a pre-amplifier (60 dB gain with a frequency range of 300–1000 kHz) and then channelled to an rms-meter that in turn outputs the signal in the form of a voltage which is sent to the computer through the same data acquisition board discussed earlier.

The loaded sample was carefully brought into contact with the rotating disc after the motor has accelerated and reached the constant pre-set speed. The data acquisition process is started few seconds prior to the actual contact between the two tribo-elements. The tribometer was enclosed during testing in a plexiglass box for safety reasons but also to maintain the relative humidity of the environment to a value close to 50% and the temperature close to 22 °C (72 °F).

After each test, the wear scar of the ball as well as the wear track of disc were observed by an optical microscope (in some cases SEM examinations were performed). The diameters of wear scar d_1 and d_2, along and perpendicular to the sliding direction, were measured with a resolution of $\pm 5\ \mu$m. These measurements enabled the determination of the wear volume of the ball according to the following equation:

$$w = \frac{\pi d_1^2 d_2^2}{64R} \tag{1}$$

in which, R is the ball radius (6.35 mm).

Three different materials were considered in this study namely: silicon nitride (Si_3N_4) in the form of commercially available balls and discs, alumina (Al_2O_3) in the form of commercially available balls as well as SAE52100 steel in the from of in-house machined and heat-treated discs. The specifications along with pertinent properties of these materials are reported in Table I.

The following mating combinations were investigated: Si_3N_4/Si_3N_4, Al_2O_3/Si_3N_4, Si_3N_4/SAE52100 steel and Al_2O_3/SAE52100. As pointed out earlier, any tested combination will be referred to hereafter by the two considered materials the first being always the ball (sample) the second being the disc.

Before testing all samples were placed into a beaker containing a 1 to 1 mixture of iso-octane and iso-propyl alcohol then put into an ultrasonic cleaner for 15 min. After they were rinsed with acetone and dried, they were stored in a desiccator. Special care was taken in order to ensure that the tribosurfaces were not contaminated when removed from the desiccator and mounted onto the testing apparatus.

3. Results and discussion

Many preliminary tests under similar conditions to those already available in the literature especially for steel on steel in dry and lubricated environments were performed in order to verify the accuracy of the results

TABLE I Specifications and pertinent properties of the samples

	Si_3N_4	Al_2O_3	SAE52100
Ball (ceramic)	Diameter 12.7 mm (1/2 in.), sphericity 0.6 μm, diameter tolerance ± 2.5 μm, maximum surface roughness $Ra = 0.05$ μm. These were sed as received from the manufacturer.		
Disc	External diameter: 50 mm, diameter of centred hole for holding purpose 25 mm, thickness 8.5 mm, contacting surface grinded then polished according to Buehler Dialog Method #10.01 to a maximum surface roughness $Ra = 0.05$ μm.		Same dimensions as ceramic discs, polished according to standard method for grain size determination to a maximum surface roughness $Ra = 0.04$ μm.
Chemical content	8% Y_2O_3, less than 0.5% Al_2O_3	99.95% Al_2O_3	Close to 1.0% C, 1.5% Cr, 0.25% Ni, 0.35% Mn, 0.1% Mo.
Hardness	15.5 GPa (from Vickers test)	17 GPa (from Vickers test)	61 to 64 Rockwell C obtained through appropriate heat treatment of austenitizing, quenching then tempering.
Elastic modulus	310 GPa	400 GPa	205 GPa
Poisson's ratio	0.24	0.26	0.33

obtained following the present experimental procedure. Fine tuning of the apparatus and data acquisition system was also conducted until satisfactory reproducibility of phenomena, generally observed for similar tribological systems, and experimental results were obtained after a reasonable number of trials carried out at repeated testing conditions. All data subsequently reported are average values derived from repeated tests whose number was increased if repeatability was not found to be satisfactory.

3.1. Time dependance of dynamic coefficient of friction and acoustic emissions

As pointed out in the introduction section, the interest of some researchers has so far mainly focussed on the correlation between acoustic emission signals (AE) and wear mechanisms or wear volume with very limited published findings about its possible relationship with friction. Therefore, it was decided first to try to find out if there was any relationship that did exist between the time dependent variation of AE and the dynamic coefficient of friction (COF). In this study, the friction coefficient was determined directly as the ratio of the simultaneously measured friction force and the instantaneous normal load. The abbreviation AE refers to the acoustic emission rms output voltage which was measured according to the schematic diagram of the acoustic emission equipment also depicted in Fig. 1.

The data of Fig. 2 were chosen as an example to illustrate the time variations of both these parameters for all four considered material combinations tested at the same conditions of normal load = 10 N, sliding speed $v = 0.1$ m/s and test duration $t = 5000$ s (equivalent to a sliding distance $s = 500$ m). Fig. 2 shows clearly that distinct patterns characterise each material combination. The depicted data suggest that there is no evidence of the existence of the three noticeable characteristic states (running-in, steady state, catastrophic damage) that distinguish the variation of the COF with respect to sliding distance, in the case of metal to metal contact [7], when ceramics are involved even when in contact with steel. At the same time, these data show that COF is not constant and that no peak generally associated with the running-in period was detected at a data acquisition frequency of 10 Hz, as it was also reported by Czichos *et al.* [8]. Instabilities of the interfacial conditions that translate to frequent seizures and releases (stick-slip phenomenon) produce marked variations of the magnitude of COF with time. Furthermore, the AE variation gives a clear indication that there is no relationship between the frequency of appearance of these peaks and any quantifiable property of the surface which may have created them. In addition, there is no apparent link between the friction and AE behaviour as function of sliding time, and it is believed that the information contained in AE variations is more related to wear mechanisms occurring in rubbing contacts as found by Boness *et al.* [9]. Finally, the present results demonstrate that drastic changes in the phenomena taking place at the interface of contact happen when Al_2O_3 is involved as the mating material as indicated by the AE variations.

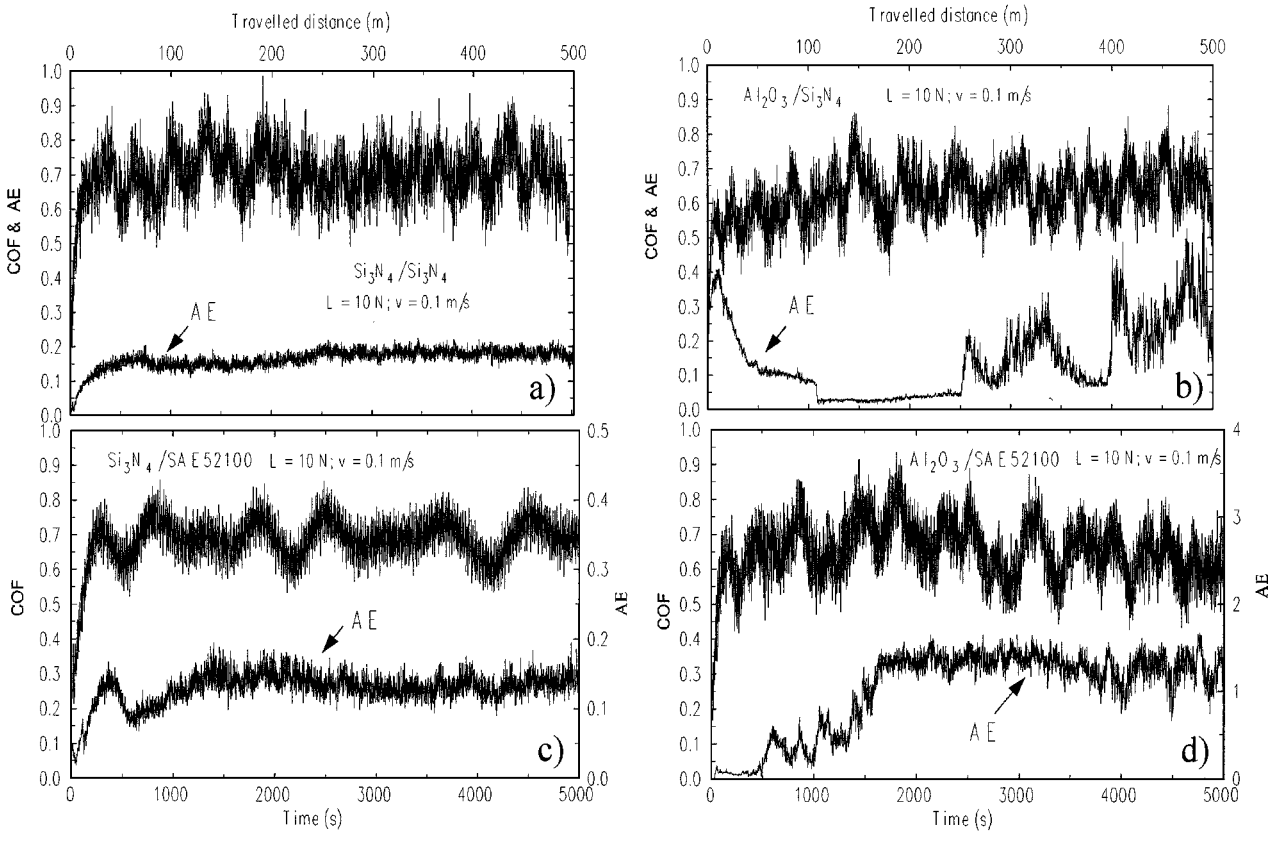

Figure 2 Variations of AE and COF with respect to testing time.

3.2. Stress analysis at the contact region

The contact stress distributions can affect the crack initiation process and further propagation leading to wear, especially in the case of sliding contact where surface fatigue takes place. Hamilton and Goodman [10] have considered the sliding contact between a sphere and a flat surface, simulated by a circular contact region carrying a hemispherical Hertzian normal pressure and a proportional distributed shearing traction. Using an analytical approach, they developed all equations necessary to define the complete stress field for the surfaces inside and outside the contact zone. These equations were used here in order to determine the state of stress at points of the contacting surface during sliding for Si_3N_4/Si_3N_4, $L = 10$ N, $v = 0.1$ m/s using an average value of COF $= 0.65$. The required mechanical properties were take from Table I. The initial (static state) radius of the circle of contact and maximum pressure at the centre of contact, adopted in these calculations were found to be: $a_0 = 0.067$ mm and $P_0 = 1058$ MPa. Briefly, these data taken as an example, showed the emergence of an important tensile stress at the onset of the contact zone. In order to investigate the impact of these stresses on the eventual failure of the surface, the von Mises stress in a Cartesian form was also evaluated. A maximum value of 1570 MPa was obtained for this case which is a clear indication that at least localized plastic deformation occurs at that location.

3.3. Coefficient of friction as function of sliding speed and normal load

These results are depicted in Figs 4 and 5 and each data point represents an average value obtained from the variation of COF over a constant sliding distance of 500 m considering at least two consecutive tests performed at either a constant nominal load of 10 N (for the tests at different sliding speeds) or sliding speed of 0.1 m/s (for the tests at different normal loads). Values of COF varying from about 0.5 to 0.9 were found depending on the material combination and the sliding speed which varied from 0.05 to 2.5 m/s. Fig. 3 shows that in all combinations except Si_3N_4/Si_3N_4 an increase of COF takes place reaching a peak value at about 0.5 m/s, followed by a substantial decrease at higher sliding speeds. Conversely, in the case of self-mated couple Si_3N_4/Si_3N_4 the increase is followed by a steady state characterized by a higher value of COF. The decrease of COF could be explained by the formation of oxides at the interface of contact, that act as "artificial lubricants", as a consequence of tribochemical reactions activated by the interfacial increase of the temperature with the sliding speed. Similar behaviour has been reported by Woydt and Habig [11] for self-mated ZrO_2. The decrease of COF at higher speeds is also evident in the results obtained by Usami *et al.* [12]. Finally, it should realised that the low values of COF quoted in the literature were generally obtained at lower sliding speeds and shorter test durations.

On the other hand, for the tests conducted at different loadings, a very clear decrease of COF with increasing normal load is indicated by the data of Fig. 4 for all four

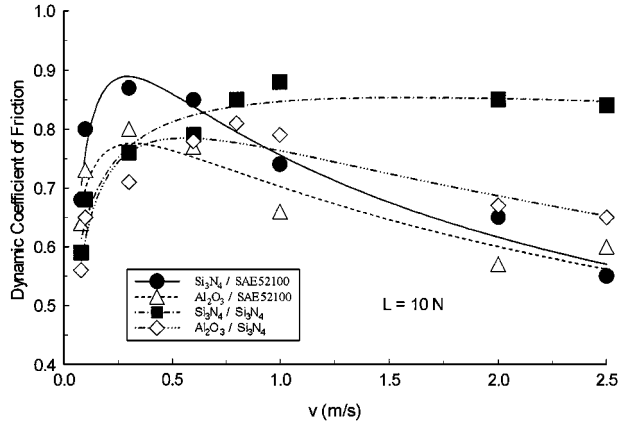

Figure 3 Relationship between sliding speed and COF for all combinations.

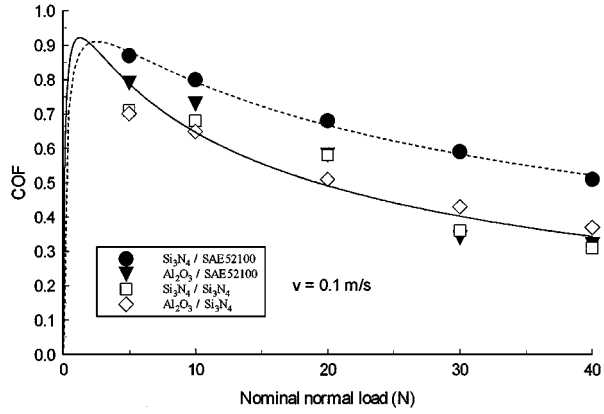

Figure 4 Relationship between normal load and COF for all combinations.

material combinations, reaching values as low as 0.3 at $L = 40$ N. In general, for the case of Si_3N_4/SAE52100 system higher values of COF ranging from 0.9 to about 0.5 were found. As can be see from Fig. 4, all data could be associated with two distinct groups of results and therefore two separate models were considered to best fit these data with reasonable accuracy, as shown by the solid and dashed lines in the figure. For loads lower than 5 N, only predictions obtained from these models are shown. This curve fitting has permitted to derive the following empirical equations:
For Si_3N_4/Si_3N_4:

$$\mathrm{COF} = 0.85L^{(0.14 - 0.07\ln(L))} \tag{2a}$$

For the remaining materials combinations:

$$\mathrm{COF} = 0.92L^{(0.04 - 0.08\ln(L))} \tag{2b}$$

3.4. Wear properties

The interest was first focussed on the investigation of the time variation of the wear volume. It is important to note that fresh contact conditions for every experimented sliding distance was preferred rather than assessing the variation of the same wear scar which requires interruptions of testing for the measurement of its corresponding dimensions to a considered sliding distance. The later procedure requires also special care

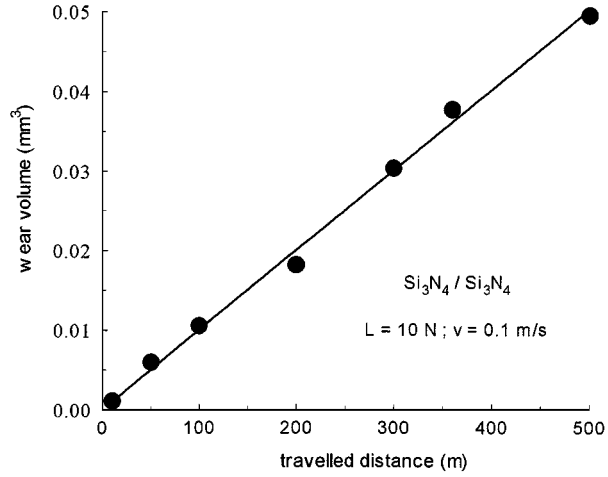

Figure 5 Wear volume of the ball for Si_3N_4/Si_3N_4 as function of sliding time.

in order to ensure that the integrity of the contact is preserved when the sample (ball) is placed back into the tribometer after the evaluation of the wear scar. It should also be pointed out that the wear damage of the disc, in terms of material loss (groove formation), was insignificant in the case of the present study and therefore was not taken into account in the evaluation of the wear volume. Self-mated Si_3N_4 couple was selected as reference to investigate this process of progression of wear as function of time at constant load and sliding speed. To that end, the average wear volume of the ball was evaluated considering three consecutive tests, each conducted at $L = 10$ N and $v = 0.1$ m/s. The variation of the average values of this parameter as function of sliding distance is illustrated in Fig. 5. These results demonstrate that a relationship of proportionality exists between these two parameters despite the effect of the related net pressure decrease during testing.

The wear rate and wear coefficient were used to compare the wear properties for each tribosystem. The first parameter is defined as usual by the following equation:

$$k = \frac{w}{Ls} \tag{3}$$

in which w is the wear volume, L the normal load and s the sliding distance. The non-dimensional form of k, commonly called wear coefficient K, is obtained by normalisation using the indentation hardness (at room temperature) according to the following equation:

$$K = kH \tag{4}$$

in which H is the indentation hardness expressed in the form of a stress.

The log-log plot in Fig. 6 displays a stronger influence of the sliding speed v on k (which is evaluated here from the wear volume of the ball only) when Al_2O_3 is involved as mating material (Al_2O_3/Si_3N_4 and Al_2O_3/SAE52100). Also a closer look at the data suggests that evident wear transitions occur for these same combinations, generally interpreted by changes in wear mechanisms. The relationship between these

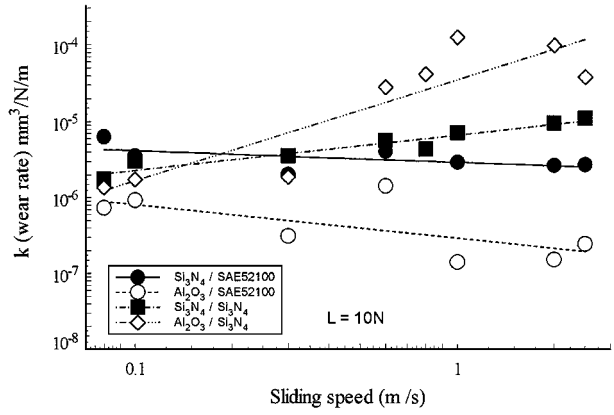

Figure 6 Influence of sliding speed on wear rate.

two parameters was found however not to be consistent for all combinations. The same behaviour is also valid in the case of K. It should be emphasized that at higher speeds the testing time was obviously shortened to keep the total sliding distance (500 m) the same for each experiment and that the point contact present at the beginning of the test expands to a flat contact area as wear progresses which would contribute to a drop of the contact pressure as function of time. These two phenomena have certainly an impact on the reported results but the recognized tribo-oxidation as predominant wear mechanism at high speed and room conditions could explain the increase of k with v for the case of mated ceramic materials. According to our results the combination Al_2O_3/SAE52100 is the most advantageous giving a value of k slightly higher than 10^{-7} $mm^3/N/m$ at high speed, on the contrary Al_2O_3/Si_3N_4 performed the poorest especially at speeds higher than about 0.3 m/s in which case k reached values as high as 10^{-4} $mm^3/N/m$.

Different behaviour and trends take place when wear tests were conducted at different nominal loads, ranging from 5 to 40 N and constant sliding speed $v = 0.1$ m/s as reported in Fig. 7. The tendency of slight decrease of k with L is fairly evident for all material combinations with the exception of Al_2O_3/SAE52100 that shows a more noticeable increase. The decrease of k is in agreement with the decrease of COF as function of the normal load, which was presented earlier. Optical observation of the surface revealed that a plowing effect was more

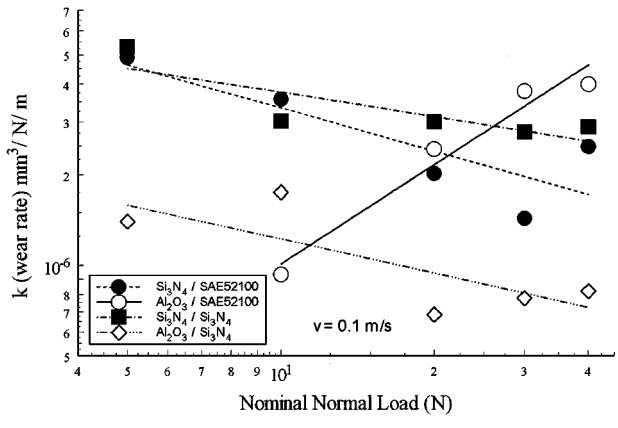

Figure 7 Influence of nominal normal load on wear rate.

evident in the case of Al_2O_3/SAE52100 combination.

In general, the microscopic morphology of the worn surfaces has revealed that in all cases, polishing and groove formation were the main transformations of the contacting surface.

3.5. Relationship between AE, wear, friction work and material removal power

Despite the serious interest and considerable effort to find a way in incorporating AE techniques in tribological applications, there is still no firm conclusions as to whether or not useful correlation could be established between AE and wear. For example, Belyi *et al.* [13] have determined that AE energy is illustrative of the wear expressed as mass loss in the case of polymer-metal friction pairs. Empirical models between integrated AE rms and wear volume have also been developed for steel on steel systems [6]. On the other hand, there are suggestions of the existence of close relationship between AE and friction work from sliding contact of pairs of materials. In this section an attempt is made to investigate the possibility of identifying any useful relationships between integrated AE rms, wear, friction work and material removal power for the case of the tribosystems considered in this study in which ceramic materials are involved. These parameters are defined by the following equations:

Integrated AE rms

$$\text{int AE} = \int (\text{AE rms signal})\, dt \tag{5}$$

Fiction work

$$F_w = \int F(t)\, ds \tag{6}$$

which is the real time variation of the friction force during testing $F(t)$, integrated with respect to the total sliding distance.

3.5.1. Material removal power

The energy required to remove a certain volume of material, approximated here by the wear volume w can be estimated by the following equation, proposed initially by Shaw [14]:

$$E = wH \tag{7}$$

in which H is the hardness. On the other hand the product (wH) can be related to the wear coefficient K using Equation 4 as: $wH = KLs$ and knowing that the power is the derivative of the energy with respect to time one can obtain the material removal power P as follow:

$$P = KLv \tag{8}$$

As shown in Fig. 8, reasonably good correlations exist between the wear rate k and int AE represented by empirical equations, each in the form of a power law whose constants are included in Table II. These results reveal the occurrence of a rather surprising phenomenon causing the decrease of k with the increase of the AE integrated rms signal that was detected in the case of sliding ceramic pairs, as evidenced by the negative values of n reported in Table II. The most plausible explanation is the predominant effect of testing time which decreases with the increase of speed, as these experiments were performed at fixed sliding distance.

The justification for modelling of wear volume and material removal power as function of the integrated AE signal with straight lines is evident from Fig. 9 that depicts the results for Si_3N_4/Si_3N_4 obtained at constant load, different sliding speeds (whose trend is indicated on the figure) and fixed sliding time of 1000 s. On the contrary, there was no readily tangible evidence of any coherent relationship between w and int AE nor between the frictional work dobe F_w and int AE according to the data obtained from the experiments conducted at the considered range of sliding speeds, fixed sliding distance (500 m) and normal load of 10 N. Widely

TABLE II Values of the constants for the power law relationships between k and int AE

	$k[\text{mm}^3/\text{N/m}] = c(\text{int AE})^n$	
	c	n
Al_2O_3/SAE52100	1.25×10^{-10}	1.23
Si_3N_4/SAE52100	11×10^{-7}	0.183
Si_3N_4/Si_3N_4	38×10^{-5}	−0.72
Al_2O_3/Si_3N_4	2.56	−2.13

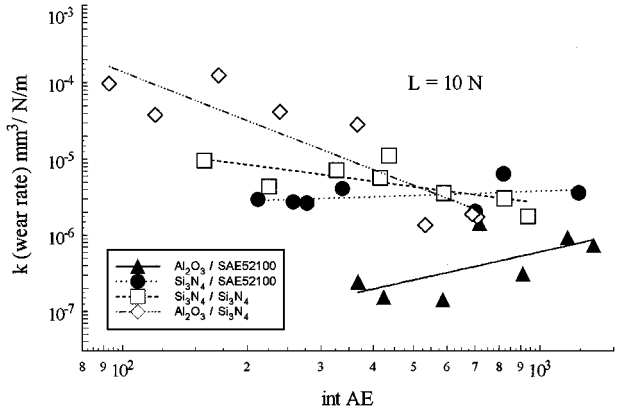

Figure 8 Relationship between wear rate and int AE.

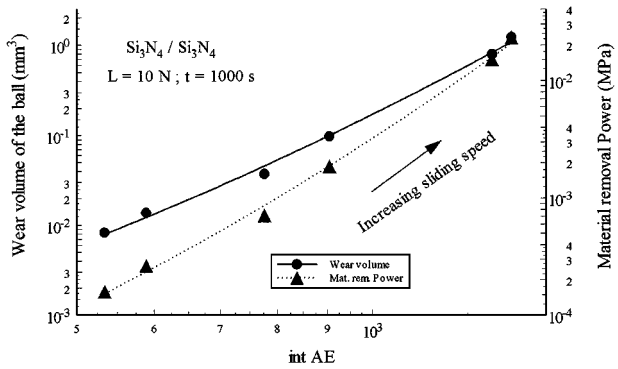

Figure 9 Wear volume and material removal power as function of int AE for Si_3N_4/Si_3N_4.

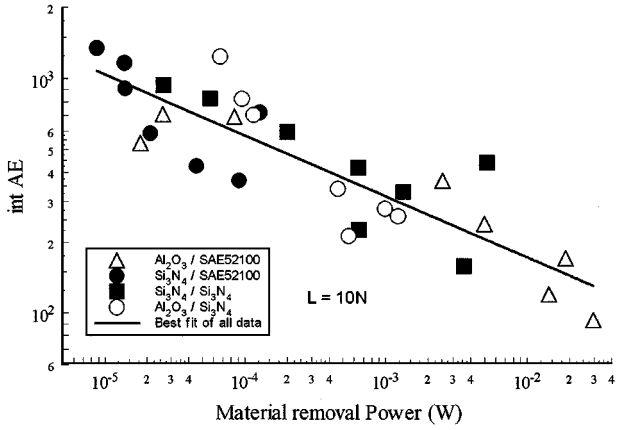

Figure 10 int AE as function of material removal power for the experiments conducted at different sliding speeds, same normal load of 10 N.

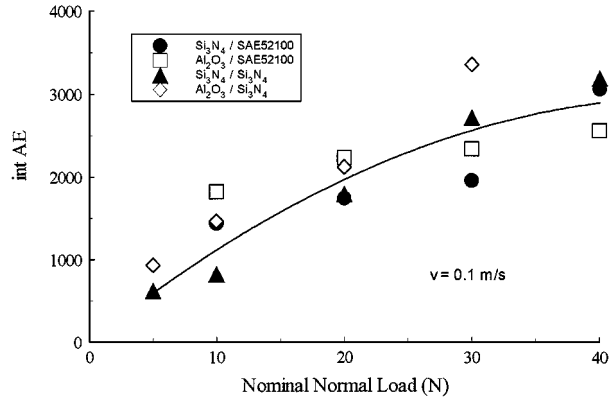

Figure 11 int AE as function of nominal normal load at constant speed of 0.1 m/s.

scattered points which appeared in random distribution characterised the plots of these data that we chose not to include in this paper. Furthermore, when all these data are summarized as shown in Fig. 10 a decrease of int AE with the material removal power P was observed. This unexpected behaviour could be attributed, once more, to the effect of shorter testing time at higher sliding speeds which also suggests that the shear strain associated with plastic deformation of the rubbing surfaces is in this case more predominant than the material removal process, the later being associated with the generation of higher Ae signals. One should anticipate a decrease of int AE for smaller values of P than those obtained in this study.

At constant speed of 0.1 m/s (constant test duration of 5000 s equivalent as before to a sliding distance of

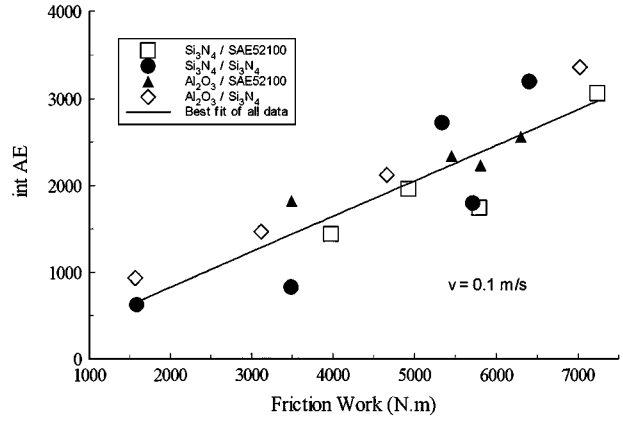

Figure 12 int AE as function of friction work at constant speed of 0.1 m/s.

500 m) a consistent increase of int AE with L was found for every tested material combination. Based on Fig. 11 that illustrates all obtained data for the experiments conducted at different normal loads, the following empirical equation in the form of a second order polynomial best fit forced through the origine was derived:

$$\text{int AE} = 124L - 1.32L^2 \tag{9}$$

Contrary to the earlier drawn conclusion based on the results pertaining to variable sliding speed conditions, the data derived at variable normal loads (fixed speed of 0.1 m/s allowing a fixed test duration of 5000 s), that permitted to construct Fig. 12, show the existence of a reasonable correlation between int AE and F_w that could be approximated by a linear relationship having a proportionality constant of 0.41. It is at this stage pertinent to mention the work of Lingard and Ng [15] who found a systematic relationship between cumulative AE count and frictional work, using disc on disc (one fixed) configuration to conduct dry friction experiments at a wide range of tribological conditions on six different metallic materials.

Furthermore, some meaningful behaviour is reflected by the plots of Fig. 13 that represents the variation of each of the two parameters of interest, the material removal power P and wear volume w, as function of the int AE. The tribo-elements are identified by the legend of the graph and all dashed lines and filled symbols pertain to the data illustrating the variation of w. Although all results show an increase of P and w with int AE, a more accentuated trend applies to the Al_2O_3/SAE52100

TABLE III General form and values of the constants for models representing the correlations between P and int AE as well as w and int AE

	$w[\text{mm}^3] = c_1(\text{int AE})$, $P[W] = c_2(\text{int AE})$	
	c_1	c_2
Si_3N_4/SAE52100	2.78×10^{-9}	1.405×10^{-5}
Si_3N_4/Si_3N_4	3.38×10^{-9}	1.69×10^{-5}
Al_2O_3/Si_3N_4	1.4×10^{-8}	4.69×10^{-6}

	$w[\text{mm}^3] = (\text{int AE})^{(c_3 + c_4 \ln(\text{int AE}))}$, $P[W] = (\text{int AE})^{(c_5 + c_6 \ln(\text{int AE}))}$			
	c_3	c_4	c_5	c_6
Al_2O_3/SAE52100	−9.8	1.21	−11.93	1.34

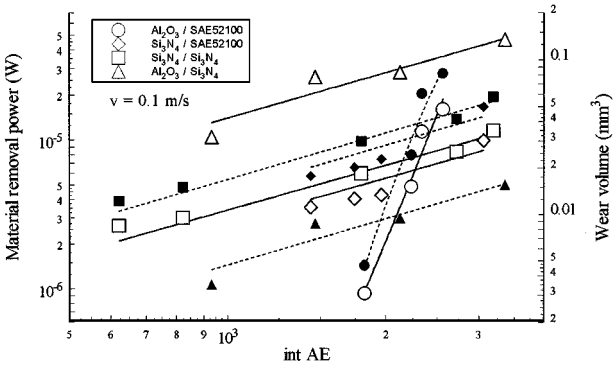

Figure 13 Material removal power and wear volume as function of int AE for all tests at constant sliding speed.

combination. This distinct behaviour was also reflected by the findings reported earlier. In order to establish relationships that could be used for predicting the tribological behaviour of similar tribo-systems, if on-line monitoring of AE signal is possible, these data were expressed in the form of either a linear equation or power law. Table III summarizes the general form of these empirical models that best fit the experimental data, which were forced to go through the origin of the graph for physical meaning, a well as the corresponding values of the constants that apply to each tribo-element.

3.6. Microscopy

Examinations of ball scars and disc wear tracks revealed a broad range of differences in appearance when the effects of the experimental conditions on the worn surfaces were assessed using optical microscopy at different magnifications. In the case of the wear ball scars the most common observed transformation was the result of polishing process that occurs at the early stage of sliding followed by a mixed behaviour with some central rough areas characterized by deep grooving arising from the combination of abrasion and transfer of material mechanisms. The pairing with like materials, i.e., Si_3N_4/Si_3N_4 was chosen to illustrate briefly these somewhat complicated and difficult to quantify phenomena that occur fairly randomly. A constant period of rubbing time of 3600 s was selected as a basis of comparison in order to investigate the individual effects of sliding speed and normal load on the appearance of the worn surface at the end of the test. Fig. 14a shows clearly the final stage of the polishing process of the ball scar that took place at a slow speed of 0.05 m/s and load of 10 N. At higher speeds of 0.3 and 0.6 m/s ($L = 10$ N) whose results are depicted by the photographs of Figs 14b and c combinations of rough track portions, darkly coloured on the pictures and smoother regions become evident. According to the early reported results, the above described processes seem not to have a significant impact on the COF and wear rate as evidenced by the fairly constant values of these two parameters obtained at different sliding speeds, when grooving and material transfer mechanisms become predominant. Different transformations occur when the load is increased (sliding speed kept constant) during which smoothing of the surface prevails as shown by Figs 15a and b for loads of 20 and 40 N ($v = 0.1$ m/s) suggesting the predominance of the mechanism of adhesion which would explain the decrease of COF with load reported earlier.

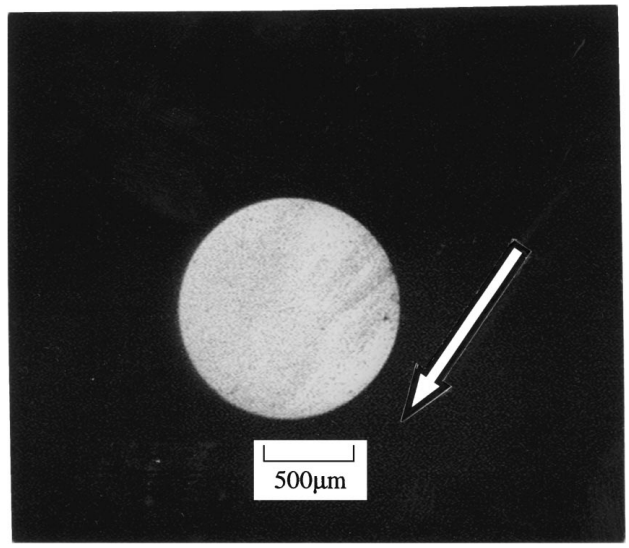

(a)

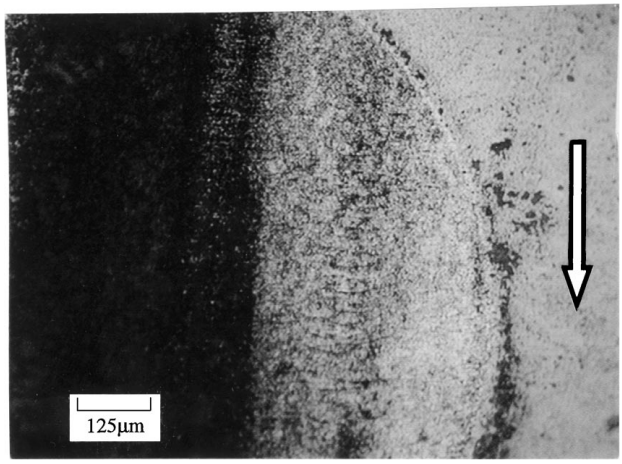

(b)

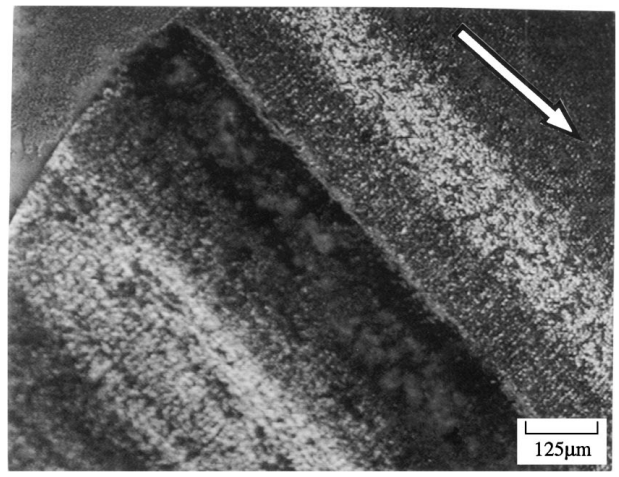

(c)

Figure 14 Photograph of the ball wear scar for Si_3N_4/Si_3N_4 system: (a) $v = 0.05$ m/s, $L = 10$ N, $t = 3600$ s, arrow showing the direction of the sliding disk, (b) $v = 0.3$ m/s, $L = 10$ N, $t = 3600$ s, arrow showing the direction of the sliding disk, and (c) $v = 0.6$ m/s, $L = 10$ N, $t = 3600$ s, arrow showing the direction of the sliding disk.

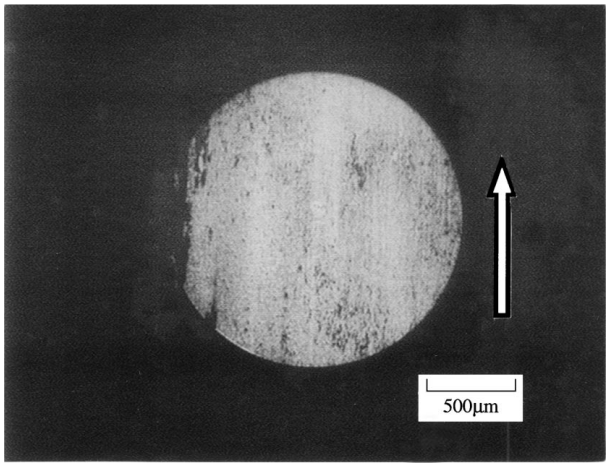

(a)

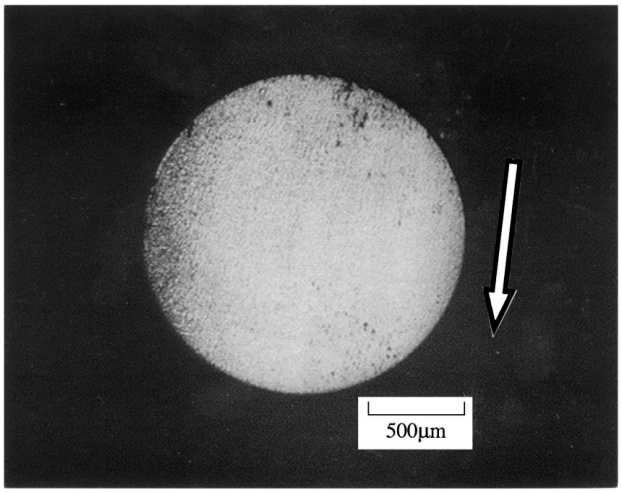

(b)

Figure 15 Photograph of the ball wear scar for Si_3N_4/Si_3N_4 system: (a) $v = 0.1$ m/s, $L = 20$ N, $t = 3600$ s, arrow showing the direction of the sliding disk, (b) $v = 0.1$ m/s, $L = 40$ N, $t = 3600$ s, arrow showing the direction of the sliding disk.

4. Conclusion

The aim of this study was to investigate the influence of sliding speed, normal load, test duration on the friction, wear and acoustic emission properties in the case of continuous dry sliding for four materials combinations namely Si_3N_4/Si_3N_4, Al_2O_3/Si_3N_4, Si_3N_4/(SAE52100 steel) and Al_2O_3/SAE52100. A designed ball-on-disc tribometer was used to conduct the testing. Based on the obtained results, the following conclusions can be drawn:

For all tribo-systems, the time dependence of the dynamic coefficient of friction showed marked variations but no distinct peak generally associated with the running-in period was noticed. At the same time no apparent link was found between the friction and the AE signal as function of sliding time.

An increase of the dynamic coefficient of friction reaching a peak value at a sliding speed of about 0.5 m/s followed by a substantial decrease was observed for all materials combinations except Si_3N_4/Si_3N_4 that showed a steady state situation. On the other hand, a clear decrease of the dynamic coefficient of friction takes place with the increase of the normal load.

The present results display a stronger influence of the sliding speed on the wear rate, as well as wear coefficient, when Al_2O_3 is involved as mating material (Al_2O_3/Si_3N_4 and Al_2O_3/SAE52100). The experimental results also suggest that evident wear transitions, generally interpreted by changes in wear mechanisms, occur for these same combinations.

Reasonably good correlations between the wear rate and the integrated AE rms signal were developed, but surprisingly a decrease of k with int AE was detected in the case of sliding ceramic pairs based on the tests conducted at different sliding speeds and constant sliding distance.

There was no readily tangible evidence of any coherent relationship between the wear volume and int AE nor between the frictional work done and int AE according to the data obtained from the experiments conducted at the considered range of sliding speeds, fixed sliding distance (500 m) and normal load of 10 N. On the contrary, the data derived at variable normal loads (fixed sliding speed and test duration) showed the existence of a reasonable correlation between int AE and the friction work, that was approximated by a linear relationship having a proportionality constant of 0.41.

Relationships that could be used for predicting interesting tribological behaviour of practical applications based on similar tribo-systems, if on-line monitoring of AE signal is possible, were expressed in the form of either a linear equation or power law for each materials combination.

Acknowledgements

The authors acknowledge the preliminary testing conducted by Dr T. Liu.

References

1. C. S. YUST, Wear of advanced ceramics, in Proc. Int. Tribology Conf. of Japan, Nagoya 1990, p. 657–661.
2. Y. BERTHIER, M. GODET and M. BRENDLE, *Tribology Trans.* **32** (1989) 490–496.
3. J. K. LANCASTER, Y. MASHAL and A. G. ATKINS, *J. Phy. D* **25** (1992) 205–211.
4. J. DENAPE and J. LAMON, *J. Mater. Sci.* **25** (1990) 3592–3604.
5. C. L. JIAA and D. A. DORNFELD, *Wear* **139** (1990) 403–424.
6. R. J. BONESS and S. L. MCBRIDE, *ibid.* **149** (1991) 41–53.
7. H. CZICHOS, *Tribology* (Elsevier, Amsterdam, 1978).
8. H. CZICHOS, S. BECKER and J. LEXOW, *Wear* **135** (1989) 171–191.
9. R. J. BONESS, S. L. MCBRIDE and M. SOBCZYK, *Tribology International* **23**(5) (1990) 291–295.
10. G. M. HAMILTON and L. E. GOODMAN, *J. of Applied Mechanics, Trans. of ASME* **33** (1966) 371–376.
11. M. WOYDT and K.-H. HABIG, *Tribology international* **22**(2) (1989) 75–89.
12. H. USAMI, K. FUNABASHI and T. NAKAMURA, Frictional properties of several kinds of ceramics against hardened carbon steel, in Proceedings of the 5th international congress on tribology, Helsinki 1989, p. 94–99.
13. V. A. BELYI, O. V. KHOLODILOV and A. I. SVIRIDYONOK, *Wear* **69** (1981) 309–319.
14. M. C. SHAW, Metal cutting principles, 3rd edition, MIT Press, 1954.
15. S. LINGARD and K. K. NG, *Wear* **130** (1989) 367–379.

Received 21 October 1998
and accepted 23 March 1999